

Diffractive shaping of excimer-laser beams for pulsed laser deposition

V. Kekkonen

Department of Applied Physics, Aalto University, P.O.Box 15100, FI-00076 Aalto, Finland

A. Hakola

VTT Fusion and Plasma Technology, P. O. Box 1000, FI-02044 VTT, Finland

T. Kajava

Timo.Kajava@tkk.fi

Department of Applied Physics, Aalto University, P.O.Box 15100, FI-00076 Aalto, Finland

We present a beam-shaping system for a pulsed laser deposition setup. This system is based on two diffractive beam-splitter gratings and is able to produce $2 \times 2 \text{ mm}^2$ flat-top distributions of UV light with a fluence of 3 J/cm^2 on the target some 30 cm behind the system. We have applied the setup to deposit ferromagnetic Ni-Mn-Ga films. [DOI: 10.2971/jeos.2011.110135]

Keywords: Flat-top profile, top-hat profile, beam-splitter grating, partial coherence

1 INTRODUCTION

Pulsed laser deposition (PLD) is a method to produce thin films from a wide range of materials (see, e.g., Ref. [1]). The technique is based on interaction of high-power laser pulses with matter in a vacuum chamber as shown in Figure 1. When pulses with a sufficiently high energy density (fluence of the order of 1 J/cm^2) interact with the thin surface layer of the target, the interaction leads to emission of particles. Typically, a visible plasma plume appears. This phenomenon is commonly referred to as laser ablation. In PLD, the emitted particles condense on a substrate placed opposite to the target to form a film. To ensure a stoichiometric film of a multicomponent material, the deposition parameters such as the fluence, background gas and its pressure, and the substrate and its temperature, need to be optimized. In addition, the spatial intensity distribution of the laser beam on the target should be homogeneous with steep edges so that the ablation threshold fluence for each component is exceeded everywhere in the interaction area. The fluence of such a flat-top profile is well defined across the whole laser-spot area so that uniform erosion of the target and smooth film surfaces are possible.

As sources of high-energy UV pulses, excimer lasers are commonly utilized in PLD applications. They do not, however, produce pulses with the ideal flat-top profile and, furthermore, the shape of the intensity distribution typically fluctuates from pulse to pulse. Another unwanted feature is that the profile tends to become inhomogeneous due to gas aging. For these reasons, beam shaping and homogenization of excimer laser beams is necessary before they can be applied in PLD. The standard way is to select the homogeneous part of the beam utilizing apertures and image it on the target plane with proper demagnification to reach the required fluence levels (Figure 2). Despite the relatively good flat-top profile that can be obtained, the method suffers from very high losses, up to 80%. The method is also unable to deal with pulse-to-

pulse fluctuations or residual inhomogeneities in the original intensity distribution. Diffractive optics, for its part, is a powerful tool for beam shaping, and it has already been utilized in beam-homogenization applications based on random-phase plates [2] and microlens arrays [3]. One major advantage of diffractive optics is that the whole beam can be utilised in producing the flat-top. However, using diffractive optics to realize proper continuous distributions is not straightforward because, due to interference effects, the setup may be very sensitive to alignment or to the incident distribution [4].

We have developed techniques suitable for partially coherent beams. In particular, we have studied a method based on diffractive beam-splitter gratings that produce a finite number of equal-intensity diffraction orders [5, 6]. Here we have taken the final step and implemented such a set up to our PLD system. An important issue here is how this technique can be ap-

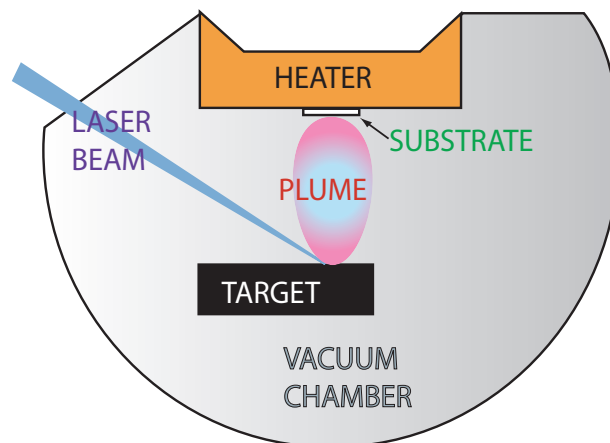


FIG. 1 Schematic illustration of the pulsed laser deposition technique.

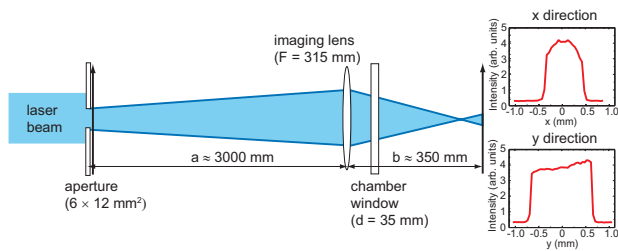


FIG. 2 Principle of a commonly used method to generate flat-top profiles in a PLD system with an excimer laser. By utilizing an aperture, the homogeneous part of the beam is imaged on the target plane. Here the demagnification of 8.6 corresponds to a fluence of approximately 5 J/cm^2 . A relatively good flat top-profile can be obtained as shown by the measured intensity profiles averaged over several pulses. The laser source is Lambda Physik COMPex 205.

plied to form mm^2 -size flat tops with high fluence a few tens of centimeters behind the beam shaping optics.

2 FLAT-TOP GENERATION WITH BEAM-SPLITTER GRATINGS

Our beam-shaping method is based on two orthogonal fan-out elements that produce a finite two-dimensional matrix of equal-intensity diffraction orders [5, 6]. Figure 3 illustrates the method in one dimension. When adjacent orders are partially overlapped in the focal plane of a positive lens, a flat-top distribution results. Disturbing interference effects can be avoided because excimer lasers are spatially partially coherent light sources. The fact that we use periodic elements ensures that the system is not sensitive to alignment or to the beam profile. The image is formed by overlapping several smaller images whose exact shape does not affect much the overall image.

The insensitivity to the initial beam profile makes it possible to realistically simulate the beam-shaping technique. Here, an appropriate choice for the excimer-laser beam is the Gaussian-Schell model (GSM), which includes both the Gaussian spatial distribution and the coherence properties of the laser beam. In GSM, the two orthogonal directions (x and y) can be handled separately, and the so-called cross spectral density function in one of the directions (here x) is given by [7]

$$W_{\text{GSM}}(x_1, x_2) = e^{-(x_1^2 + x_2^2)/w_0^2} e^{-(x_1 - x_2)^2/(2\sigma_0^2)}, \quad (1)$$

where w_0 is the $1/e^2$ width at the waist and σ_0 is the coherence width. The degree of spatial coherence in this model is defined as $\alpha = w_0/\sigma_0$. Because this parameter is directly related to the far-field divergence of the beam given by $\theta = \lambda/(\pi w_0 \beta)$, where $\beta = (1 + \alpha^{-2})^{-1/2}$ it can be easily determined experimentally. With a transmission grating of a period d designed to produce $2M+1$ diffraction orders the intensity distribution in the focal plane of the lens (focal length F) can then be written as [6]

$$I(u) = \frac{w_0}{w_F} \sum_{m,n=-M}^M T_m^* T_n \times \exp\{-[(u + mu_0)^2 + (u + nu_0)^2]/w_F^2\} \times \exp[-(m - n)^2 u_0^2 / (2\sigma_F^2)], \quad (2)$$

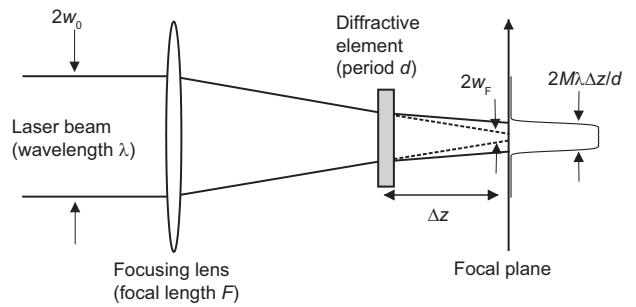


FIG. 3 A diffractive phase grating that produces a few $(2M+1)$ equal-intensity orders of a partially coherent beam forms a good approximation of a flat-top distribution when the orders are overlapped at the focal plane of a positive lens. The dotted line with the spot size of w_f denotes the propagation of the zeroth order, which is identical to beam focusing without the grating.

where T_m is the complex amplitude of the order m . The parameter $w_F = F\lambda/\pi w_0 \beta$ is the width of a single diffraction order, i.e., that of a focused spot without the diffractive grating, and $\sigma_F = \sigma_0 w_F/w_0$ is the corresponding coherence width. In the focal plane the diffraction orders have a spacing of $u_0 = \Delta z \lambda/d$.

The flat-top width in this method is determined by the number of the orders and their spacing ($W \approx M u_0$) and the edge steepness is given by the steepness of the focused spot. The simple form for the expected output profile is directly applicable to simulations to select the optimum number of orders and the grating period. These simulations give distributions which have been found to be very close to the corresponding experimental ones [6]. The fact that the initial distribution differs from a Gaussian one is not critical because the quality of the flat top does not depend on the exact shape of an individual order.

3 EXPERIMENTAL

Our goal is to shape the $12 \times 26 \text{ mm}^2$ ($x \times y$) beam of an excimer laser (Lambda Physik COMPex 205, $\lambda = 248 \text{ nm}$, pulse energy $E_p = 0.5 \text{ J}$) to a few mm^2 flat-top distribution. Since the diffractive elements cannot be placed inside the deposition chamber (distance between the target and the beam-entrance window $\sim 30 \text{ cm}$, see Figure 1), the flat top need to be produced some 30 cm behind the beam shaper optics. Another issue to take into account is that the target is tilted at an angle of $\alpha = 60^\circ$ with respect to the incoming beam so that the projected area on the target is larger by a factor of two. Yet another constraint is the diameter ($D = 35 \text{ mm}$) of the entrance window of the chamber. The goal for the fluence is 3 J/cm^2 , which is sufficient for ablating most of the relevant materials.

In practice, identical diffraction orders can be generated either by the so-called Damman gratings [8] or by continuous-relief elements. As binary diffractive elements, the Damman gratings are easier to fabricate, but their maximum diffraction efficiency to the desired orders is approximately 80%. This is an issue in high power lasers especially because it is not straightforward to design exactly in which orders the remaining 20% of the laser light goes. We therefore rely on quasi-

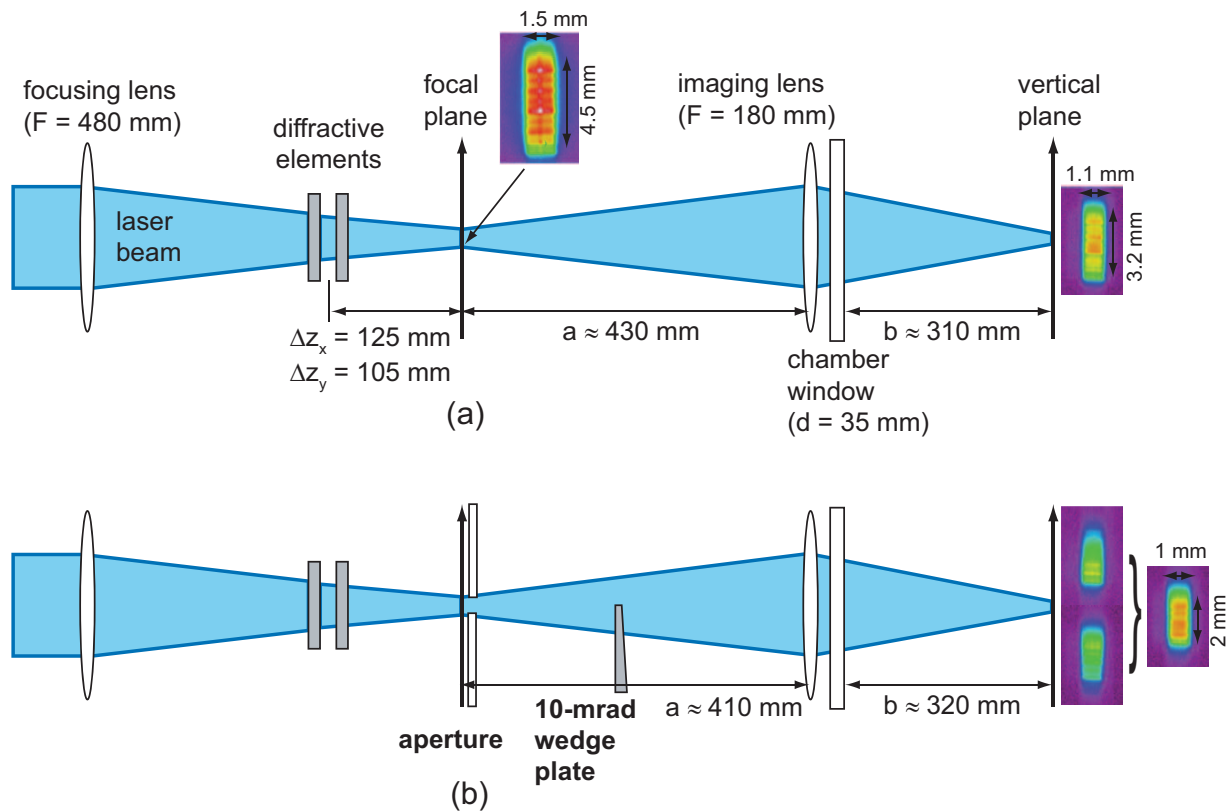


FIG. 4 (a) Two orthogonal beam-splitter gratings with periods $d_x = 200 \mu\text{m}$ and $d_y = 50 \mu\text{m}$ are able to produce a $1.5 \times 4.5 \text{ mm}^2$ ($x \times y$) flat top approximately 100 mm behind them [6]. When this distribution is imaged on the target with an $F = 180 \text{ mm}$ lens (magnification $b/a \approx 0.72$), a $1.1 \times 3.2 \text{ mm}^2$ flat top is formed on a vertical plane at the target. On the tilted target plane ($\alpha = 60^\circ$) this corresponds a $2.2 \times 3.2 \text{ mm}^2$ flat top with a maximum fluence of 2.2 J/cm^2 . (b) With a wedge plate placed between the focal plane and the imaging lens, the distribution can be split in to two trapezoidal distributions that can be overlapped on the target plane to shrink the distribution (in y -direction) and increase the fluence. An aperture was added in the focal plane to improve the steepness in the y -direction. A $2 \times 2 \text{ mm}^2$ flat top with a fluence of 3 J/cm^2 on the target plane was generated.

continuous-relief gratings, which allow much higher efficiencies although the fabrication process is more demanding. We have used ion beam lithography and proportional reactive-ion etching to produce the micrometer-sized features on the elements [9]. The phase profiles of the gratings were calculated by using a complex-amplitude transmittance approach [10].

To optimize the steepness of the flat top in our method, one should choose as short a focal-length lens as possible, which means that F should be close to 300 mm as well. This implies that the elements should be of the same size as the original beam, but the fabrication of elements with the required accuracy does not allow this. In order to transmit and withstand the energetic UV pulses, fused silica gratings are practically the only solution. For phase gratings, the groove depth is given by $h_{2\pi} = \lambda/(n-1)$, which in our case results in $h_{2\pi} \approx 500 \text{ nm}$. Here $n = 1.508$ is the refractive index of fused silica. Our simulations and test elements indicate that the average depth error across the element must be less than 2% (10 nm). This requirement limits the practical element size to approximately 1 cm^2 . Fabrication errors change the intensities of the orders; especially they tend to enhance the zeroth order.

Since we cannot produce a proper flat top 30 cm inside the vacuum chamber directly, we decided to form a good-quality flat top in front of the chamber and then image it on the target plane. We use the set up and elements of Ref. [6] with $F = 480 \text{ mm}$ and $\Delta z_x = 125 \text{ mm}$ and $\Delta z_y = 105 \text{ mm}$. From

the measured sizes of the beam before and at the focal plane of the lens ($w_{0x} \approx 150 \mu\text{m}$, $w_{0y} \approx 600 \mu\text{m}$) we obtain beam qualities of $M_x^2 = 29.6$ and $M_y^2 = 211.3$ which correspond to degrees of spatial coherence of $\alpha_x = 0.034$ and $\alpha_y = 0.0047$. The groove profiles of the gratings are optimized to produce nine equal-intensity diffraction orders because $M = 4$ maximizes the diffraction efficiency to higher than 99%. We selected the grating periods of $d_x = 200 \mu\text{m}$ and $d_y = 50 \mu\text{m}$, which correspond to order spacings of $u_{0x} \approx 150 \mu\text{m}$ and $u_{0y} \approx 500 \mu\text{m}$ at the focal plane. Note that the selected spacings are close to the widths of the orders so that partial overlap at the focal plane takes place.

In principle, both orthogonal gratings could be patterned in a single element, but the use of separate elements allows fine tuning of the flat-top dimensions by separate parameters Δz_x and Δz_y . This way the widths can be varied by some tens of a per cent without compromising the flat-top profile. More details of the gratings and their fabrication can be found in Ref. [6].

A schematic illustration of the two-stage setup with some relevant dimensions are presented in Figure 4(a). The $1.5 \times 4.5 \text{ mm}^2$ (FWHM) flat-top, produced by the gratings, is imaged with an $F = 180 \text{ mm}$ lens on the target surface (at 60° angle of incidence) some 30 cm inside the PLD chamber. This way a 7 mm^2 flat top is formed on the target plane but the maximum fluence was determined to be only 2.2 J/cm^2 ,

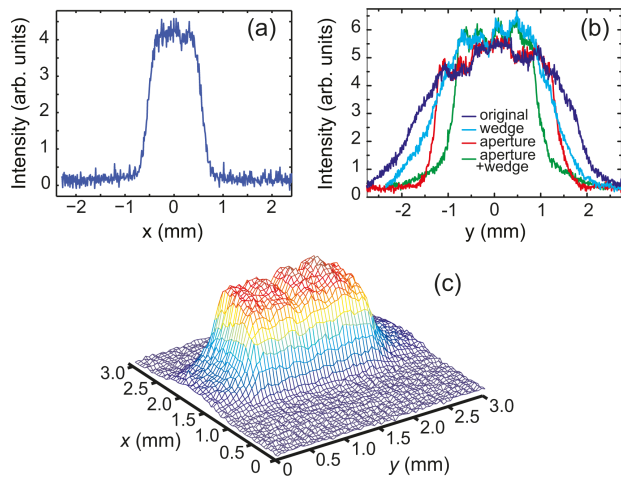


FIG. 5 (a, b) One-dimensional intensity profiles of the generated flat-top excimer laser beam. The effects of the wedge and the aperture for the y direction are individually shown. (c) The corresponding two-dimensional intensity distribution.

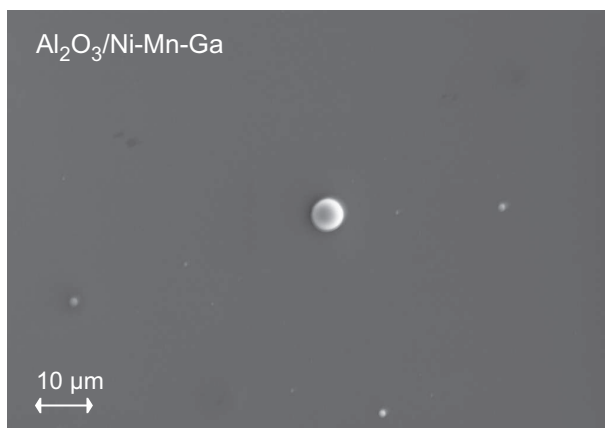


FIG. 6 LEO 1450 scanning electron microscope (SEM) image of Ni-Mn-Ga film deposited on Al₂O₃. The film surface is smooth except a single 10 μm droplet originating directly from the target.

limited mainly by the damage threshold ($\approx 2 \text{ J/cm}^2$) of the gratings [11]. We measured practically identical distributions 10 mm in front of and behind the target plane, which proves that geometrical projection of the x profile on the tilted target plane is appropriate. In principle, the image size could be further reduced, e.g., by increasing the distance a but the window size does not allow this. We thereby conclude that even with this setup we are not able to reach the goal fluence.

Figure 4(b) shows a modified setup where we added a quartz wedge plate so that half of the beam passes through the plate. Also the a and b distances were slightly adjusted. In the z direction the plate has to be placed in such a way that some of the orders in the y direction miss the wedge. This means that the object size for both the beam components is smaller than the original so that the image size is smaller as well. We selected a 10 mrad wedge plate and placed it 22 cm in front of the imaging lens to produce two trapezoidal distributions that, with the spatial adjustments of the wedge and the imaging lens, can be overlapped on the target plane to form a smaller flat top with a higher fluence. An advantage of the two-phase method is that the steepness of the profile can be

improved by adding an aperture close to the gratings. With the wedge and aperture we manipulate the beam only in the longer y direction. The modified beam shaper is able to produce a 4 mm² flat-top distribution on the target with fluences of the order of 3 J/cm². Figure 5 shows the obtained spatial profile of the beam. An rms error of 5.4% was calculated for the flat top where both the wedge and aperturing were used. Without aperturing the rms error was 6.1% and increased to some 12% when the wedge was removed as well (based on profiles of Figure 5(b)). The efficiency of the beam-shaping system is 45%, which is considerably larger than the 20% of our previous system based on imaging an apertured beam. It should be further noted that the 45% efficiency is achieved without any AR-coated surfaces.

4 PLD RESULTS

Ni-Mn-Ga alloys are ferromagnetic shape-memory compounds that can change their shape without plastic deformations up to 10% in an external magnetic field. In thin-film form, these materials enable the realization of novel micromechanical devices [12].

Substrate	Fluence (J/cm ²)	Ni (at.%)	Mn (at.%)	Ga (at.%)
Al ₂ O ₃	2.9	56	26	18
NaCl	3.0	50	25	25
Target		51.7	27.9	20.3

TABLE 1 Composition of the deposited Ni-Mn-Ga films compared to that of the target as determined by an INCA Energy 300 energy-dispersive spectrometer (EDS) and a VG Ionex IX-70S secondary ion mass spectrometer (SIMS).

We have studied the functionality of the above-mentioned beam-shaping setup by growing Ni-Mn-Ga films on Al₂O₃ and NaCl substrates. The films deposited under optimal deposition conditions are ferromagnetic with a smooth surface and with a low droplet density as Figure 6 shows. Table 1 summarizes the obtained material quality in terms of the composition of the films. Compared to the target composition, the analysis shows nearly stoichiometric deposition although the films on Al₂O₃ are slightly enriched in Ni and depleted in Mn and Ga and the films on NaCl show a higher Ga content. The results suggest that the 3 J/cm² fluence may not be high enough for depositing this material. More detailed deposition results will be presented later in another paper.

5 CONCLUSIONS

Our results demonstrate that periodic diffractive elements provide an efficient way to transform partially coherent fields into various kinds of continuous distributions. A system based on such elements is not sensitive to alignment or changes in the initial intensity distribution. Smooth profiles can be obtained because disturbing interference does not occur. Here we have integrated such a beam-shaping system into a pulsed laser deposition set-up. A 2 × 2 mm² flat-top with a fluence of 3 J/cm² was produced on the target plane some 30 cm inside the deposition chamber. Such a distribution

with steep edges and a high, well-defined fluence is ideal for PLD applications. We demonstrated this by depositing high-quality ferromagnetic Ni-Mn-Ga thin films.

The fluence levels reported here are limited by the size of the grating elements and their damage threshold. Even higher fluences can be produced closer to the beam shaper (shorter focal length of the imaging lens) or by using larger-area gratings. However, fabrication of larger elements meeting the tolerances (depth error less than 2%) is very difficult. It should also be noticed that the $2 \times 2 \text{ mm}^2$ flat top with 3 J/cm^2 at the tilted target corresponds to a $1 \times 2 \text{ mm}^2$ flat top with $> 6 \text{ J/cm}^2$ at normal incidence. In addition to PLD, such high-fluence UV flat tops are useful in other material processing applications such as drilling and micro machining of hard materials.

6 ACKNOWLEDGEMENTS

We acknowledge Prof. J. Turunen, Dr. H. Pietarinen, Dr. P. Pääkkönen, Dr. P. Laakkonen, and Dr. J. Simonen of the University of Eastern Finland, Joensuu for the design and fabrication of the diffractive beam-splitter gratings. Dr. Y. Ge of the Department of Materials Science, Aalto University, Espoo, Finland is acknowledged for the SEM and EDS analyses.

References

- [1] R. Eason, *Pulsed laser deposition of thin films – applications-led growth of functional materials* (Wiley, New Jersey, 2007).
- [2] C. L. S. Lewis, I. Weaver, L. A. Doyle, G. W. Martin, T. Morrow, D. A. Pepler, C. N. Danson, and I. N. Ross, "Use of random phase plate as a KrF laser beam homogenizer for thin film deposition applications", *Rev. Sci. Instrum.* **70**, 2116–2121 (1999).
- [3] F. Nikolajeff, S. Hård, and B. Curtis, "Diffractive microlenses replicated in fused silica for excimer laser-beam homogenizing", *Appl. Opt.* **36**, 8481–8489 (1997).
- [4] H. Aagedal, F. Wyrowski, and H. Schmid, *Diffractive Optics for Industrial and Commercial Applications* (Wiley-VCH, Berlin, 1997).
- [5] J. Turunen, P. Pääkkönen, M. Kuittinen, P. Laakkonen, J. Simonen, T. Kajava, and M. Kaivola, "Diffractive shaping of excimer laser beams", *J. Mod. Optic* **47**, 2467–2475 (2000).
- [6] T. Kajava, A. Hakola, H. Elfström, J. Simonen, P. Pääkkönen, and J. Turunen, "Flat-top generation of an excimer-laser beam generated using beam-splitter gratings", *Opt. Commun.* **268**, 289–293 (2006).
- [7] F. Gori, "Collett-Wolf sources and multimode lasers", *Opt. Commun.* **34**, 301–305 (1980).
- [8] H. Dammann, and K. Görtler, "High-efficiency in-line multiple imaging by means of multiple phase holograms", *Opt. Commun.* **3**, 312–315 (1971).
- [9] P. Laakkonen, J. Lautanen, V. Kettunen, J. Turunen, and M. Schirmer, "Multilevel diffractive elements in SiO_2 by electron beam lithography and proportional etching with analogue negative resist", *J. Mod. Optic* **46**, 1295–1307 (2000).
- [10] P. Pääkkönen, *Beam transformation and shaping by means of diffractive optics* (University of Joensuu, Department of Physics, Väisälä Laboratory, Dissertation 27, 2000)
- [11] J. Ihlemann, B. Wolff, and P. Simon, "Nanosecond and femtosecond excimer laser ablation of fused silica", *Appl. Phys. A* **45**, 363–368 (1992).
- [12] A. Hakola, O. Heczko, A. Jaakkola, T. Kajava, and K. Ullakko, "Pulsed laser deposition of Ni-Mn-Ga thin films on silicon", *Appl. Phys. A* **79**, 1505–1508 (2004).